scientific reports

Check for updates

OPEN

# Targeting *GLI1* and *BAX* by nanonoscapine could impede prostate adenocarcinoma progression

Mohammad Hossein Derakhshan Nazari[1], Ronak Heidarian[2], Mina Masoudnia[3], Rana Askari Dastjerdi[1], Parnian Ghaedi Talkhounche[4] & Sara Taleahmad[5]✉

**Prostate cancer as a critical global health issue, requires the exploration of a novel therapeutic approach. Noscapine, an opium-derived phthalide isoquinoline alkaloid, has shown promise in cancer treatment thanks to its anti-tumorigenic properties. However, limitations such as low bioavailability and potential side effects have hindered its clinical application. This study introduces nanonoscapine as a novel medication to overcome these challenges, leveraging the advantages of improved drug delivery and efficacy achieved in nanotechnology. We monitored the effects of nanonoscapine on the androgen-sensitive human prostate adenocarcinoma cell line, LNCaP, investigating its impact on *GLI1* and *BAX* genes' expressions, crucial regulators of cell cycle and apoptosis. Our findings, from MTT assays, flow cytometry, and gene expression analyses, have demonstrated that nanonoscapine effectively inhibits prostate cancer cell proliferation by inducing G2/M phase arrest and apoptosis. Furthermore, through bioinformatics and computational analyses, we have revealed the underlying molecular mechanisms, underscoring the therapeutic potential of nanonoscapine in enhancing patient outcomes. This study highlights the significance of nanonoscapine as an alternative or adjunct treatment to conventional chemotherapy, warranting further investigation in clinical settings.**

**Keywords** Noscapine nanoparticles, Cell cycle arrest, Tumor cell apoptosis, Bioinformatics

Prostate cancer is the second most common type of cancer in men globally, with approximately 1,276,106 confirmed cases and a mortality rate of 358,989 in 2018. In the U.S. alone, it accounted for an estimated 191,930 new cases and 33,330 deaths in 2020, making it the fifth leading cause of cancer-related death[1,2]. Studies have identified age, genetic predispositions such as family history, hormonal balance, and environmental factors as primary risk factors for prostate cancer[3]. Different screening programs based on biopsy, prostate-specific antigen (PSA) examination, trans-rectal ultrasound, digital-rectal examination, and using biomarkers like 8-Hydroxy-2-Deoxyguanosine or 8-Iso-Prostaglandin F2α have been developed, helping the classification of patients to low, intermediate, and high-risk groups[4–6]. This classification incorporates the choice of treatments and frequency of surveillance. The therapy line begins with prostatectomy and radiotherapy alongside active observation. At the intermediate level often Androgen deprivation therapy (ADT) is also combined[7]. In the advanced and metastatic type of prostate cancer often the first line of treatment starts with chemotherapy and ADT[8]. The development of resistance to ADT or castration-resistant prostate cancer (CRPC) or metastasis to bones could lead to a shift of treatment to chemotherapy, and poly (ADP-ribose) polymerase inhibitors alongside other treatment methods[9]. Taken together, despite the advances in treatment options and screening tools, it has not eliminated the need for making more progress in finding new therapeutic ways, and approximately 30% of patients experience recurrence[10]. Considering the necessity for chemotherapy agents as one of the main options for prostate cancer treatment, side effects, and the probable resistance to growing through receiving the treatment, it is vital to develop agents with fewer complications.

[1]Department of Microbiology and Microbial Biotechnology, Faculty of Life Science and Biotechnology, Shahid Beheshti University, Tehran, Iran. [2]Department of Developmental Biology, Kharazmi University, Tehran, Iran. [3]Department of Immunology, School of Medicine, Shahid Beheshti University of Medical Sciences, Tehran, Iran. [4]Department of Cell and Molecular Biology, Faculty of Life Science and Biotechnology, Shahid Beheshti University, Tehran, Iran. [5]Department of Stem Cells and Developmental Biology, Cell Science Research Center, Royan Institute for Stem Cell Biology and Technology, ACECR, Tehran, Iran. ✉email: s.taleahmad@royan-rc.ac.ir

Noscapine, a pthalideisquinoline alkaloid with the formula C22H23O7N, features a tetracyclic scaffold and is water-insoluble. It was first extracted from opium in 1803[11]. Since 1960, noscapine, due to its low toxicity and non-narcotic feature, has been used as an antitussive in tablets and syrup, though its effects go further. Noscapine has also been shown to have an anti-cancer activity tested on different lines of cancer cells[12,13], including prostate cancer cells[11,14]. However, interaction with warfarin and nausea and abdominal discomfort at high dosages have been reported as noscapine's intricacy[15,16]. Moreover, there are some restrictions on using noscapine, like a highly effective dose (ED50) and low bioavailability[17], which has impeded the further investigation of this treatment. Recent studies suggest nano-drugs are more efficient, offering increased safety, lower toxicity, longer blood residence times, and improved delivery and pharmacodynamics[18]. Hence, shifting to nanoscale noscapine could improve the problem facing prostate cancer.

Not only has noscapine been recognized for its microtubule-interfering feature, but also it can make a fundamental change in the expression profile of cancer cells in a way that suppresses their growth and brings them death[19]. The expression alterations of *BCL2* Associated X protein (*BAX*) and Glioma-associated oncogene-1 (*GLI1*) have been shown in previous studies to play a vital role in cancer progression making them candidates for anticancer drugs[19,20]. These genes play vital roles in cell cycle, apoptosis, and hedgehog signaling pathways[20,21]; consequently, designing a noscapine nanoparticle that impacts *GLI1* and *BAX* expression to prohibit cancer cell growth and division, which is desired in the current research, is valuable.

RNA sequencing as a high-throughput method has been widely used to monitor the mRNA expression profile in cancer research[22]. These mRNA profiles on the Gene Expression Omnibus (GEO) database could be analyzed using bioinformatics tools to screen biomarkers[23].

In the present research, we used RNA seq profile analysis and qRT-PCR to monitor the expression changes of *GLI1* and *BAX* in the LNCaP (androgen-sensitive human prostate adenocarcinoma [PRAD]) cell line before and after treating with a synthesized and characterized nanonoscapine[24]. First, an MTT assay was conducted to test the prostate cancer cells' viability confronting nanonoscapine and obtain the appropriate dose effect. Then, flow cytometry was carried out to analyze apoptosis and cell cycle in the LNCaP cells. Next, mRNA profile analysis was performed to monitor the expression of *GLI1* and *BAX* in prostate cancer before and after nanonoscapine treatment. Finally, functional annotations were executed to discover the molecular mechanism by which *GLI1* and *BAX* are contributed.

## Results

### Characterization of nanoparticles

Zeta Sizer (Malvern, UK) was used to measure the size and size distribution of the prepared nanosuspension using the dynamic light scattering (DLS) method. The diameter of the nanoparticles averaged 20 nm and the zeta potential of the particles was also measured to be −1.44 mV. Characterization of the morphology of the nanoparticles was carried out by TEM measurements. Accordingly, most of the nanoparticles were found to have a regular spherical shape under optimal conditions. Moreover, the estimated particle size was below 20 nm, which shows good agreement with the DLS results. Further analysis of the synthesized nanoparticles of noscapine is represented in Azarian M. et al. research[24].

### Dose-dependent effect of nanonoscapine on LNCaP cells

MTT assay, which was used to determine the influence of nanonoscapine on cell viability, illustrated that nanonoscapine could display a dose-dependent effect on LNCaP cells. For This cell line, at 24 h, a concentration of 100 µg/ml nanonoscapine showed nearly 50% of viable cells, and at 48 h, a concentration of 50 µg/ml nanonoscapine showed nearly 50% of viable cells (Fig. 1). Consequently, 50 µg/ml concentration was considered the appropriate dose according to possible lower side effects.

### Apoptosis induction to G2/M arrested and S phase cells

Flow cytometry data indicated that apoptosis was induced in prostate cancer cells because of nanonoscapine. The population analysis of the cells that had proceeded to apoptosis was performed with co-staining with annexin V and PI. Figure 2a illustrates the density plot and average cell percentage diagram obtained from untreated control cells and treated cells with nanonoscapine. The untreated control population of cells contained a low percentage of apoptotic cells (~ 6.65%). However, the percentage of the population of apoptotic cells after treatment with nanonoscapine reached 40.2%.

Also, to determine DNA content and cell cycle phase, flow cytometry analysis was used. Regarding cell cycle flow cytometry analysis, as expected, the population of control cells outnumbered the treated cells with nanonoscapine (Fig. 2b). However, 7% and 14% decrease in the population of the treated cells with nanonoscapine in comparison with the population of control cells in the G2/M phase and S phases, respectively, were proposing their death under the influence of the treatment and the fact that nanonoscapine could cause the cell cycle arrest in G2/M phase and induce apoptosis in cancer cells (Fig. 2c). These outcomes also indicate the nanonoscapine toxicity for prostate cancer cells.

### *GLI1* and *BAX* as the tumor suppressor genes in prostate cancer

The mRNA expression data of GSE70466 was analyzed using BioJupies to track the expression alterations of *GLI1* and *BAX* in prostate cancer. Among 5802 significant DEGs (Fig. 3a), *BAX* and *GLI1* were detected to be downregulated with FC of 0.37 and 0.247 (Fig. 3b) for prostate cancer cell growth and division, proposing an anti-tumor activity of *BAX* and *GLI1*. Furthermore, screening the transcription of *GLI1* and *BAX* before and after drug delivery at the mRNA and protein level by qRT-PCR and western blotting respectively showed that nanonoscapine enormously increased their expression by FC of 12.87 and 19.5, with $p < 0.05$ (Fig. 3c). The current

| | 0 | 12.5 | 25 | 50 | 100 |
|---|---|---|---|---|---|
| Mean | 100.0 | 73.09 | 59.29 | 48.72 | 40.59 |
| Std. Deviation | 5.076 | 2.813 | 2.207 | 1.676 | 4.953 |
| Std. Error of Mean | 2.931 | 1.624 | 1.274 | 0.9677 | 2.859 |

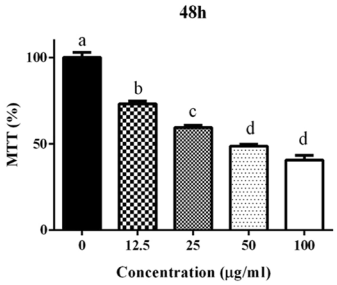


Different letters indicate significant differences between groups ($p<0.05$).

| | 0 | 12.5 | 25 | 50 | 100 |
|---|---|---|---|---|---|
| Mean | 100.0 | 86.16 | 77.16 | 66.27 | 44.35 |
| Std. Deviation | 5.123 | 8.032 | 3.541 | 3.115 | 2.858 |
| Std. Error of Mean | 2.958 | 4.637 | 2.045 | 1.799 | 1.650 |

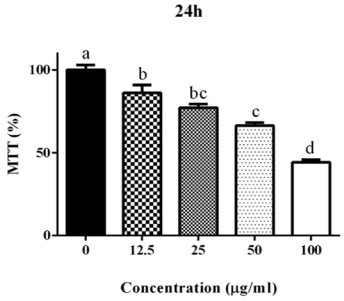


Different letters indicate significant differences between groups ($p<0.05$).

**Figure 1.** Nanonoscapine effect on LNCaP cells. Cell viability impacts of nanonoscapine in LNCaP cell line (assessed by MTT assay). Exposure of LNCaP to 12.5, 25, 50, and 100 µg/ml doses of nanonoscapine in a 24-(left hand) and 48 h (right hand) period of incubation. Bars represent the mean ± SEM of two times experiments.

observation, together with flow cytometry and MTT results, indicates a suppressor operation for *GLI1* and *BAX* that their overexpression probably leads to cell death.

## Targeting *GLI1* and *BAX* improve the survival of prostate cancer patients

The Kaplan Meier plot was constructed for *GLI1* and *BAX* using GEPIA to monitor the correlation between *GLI1* and *BAX* expression and the life expectance of prostate cancer patients. It was observed that low expression of *BAX* during the 75th to 120th month and *GLI1* after the 120th month (Fig. 3d) is related to an increase in the mortality of prostate adenocarcinoma patients. However, high expression of *BAX* before approximately the 110th month and *GLI1* before the 75th month is associated with a higher chance of survival. These outcomes suggest that overexpressing *GLI1* and *BAX* early after the prostate cancer diagnosis by nanonoscapine could improve the disease.

## Cell cycle G2/M arrest and induced apoptosis to LNCaP cells

To recognize the biological effects of *GLI1*, a member of hedgehog signaling, and *BAX*, a member of intrinsic apoptosis signaling, all DEGs were analyzed in PANTHER which showed that GLI1 is a DNA binding transcription factor (GO:0,044,212) in the nucleus (GO:0,005,634) that regulates cell proliferation (GO:0,042,127), and BAX is a mitochondrial outer membrane protein (GO:0,005,741) with homodimerization activity (GO:0,042,803) involved in regulating apoptosis (GO:0,042,981) (Fig. S1).

To further investigate the effect of GLI1 on cell proliferation and BAX on cancer cell death, several 133, 86, and 7 genes that were detected to be involved in the cell cycle (GO:0,007,049), apoptotic process (GO:0,006,915), and hedgehog signaling pathway (P00025) were obtained for further analysis (Table S2). The Pearson correlation was calculated among these genes and showed 17,654 significant co-expression interactions with the coefficient > 0.7 or < −0.07, among which 27 and 16 interactions for *GLI1* and *BAX* were verified in GEPIA and identified to be associated with cell cycle and apoptosis, respectively (Table S3). By using such interactions, two networks for *GLI1* and *BAX* were constructed in Cytoscape to generate models for studying the consequence of nanonoscapine on cell cycle and apoptosis (Fig. 4a). Then, networks were annotated in PANTHER to manifest associated molecular functions and cellular components, and *GLI1* and *BAX* revealed protein serine/threonine kinase activity and protein heterodimerization activity as signature CCs and nucleus and mitochondrial outer membrane as signature MFs (Fig. 4b).

Within *GLI1* cell cycle- and *BAX* apoptotic-interacting genes, *CDK1* and *BID* with the highest number of significant co-expressive edges (202 and 206 co-expression interactions, respectively), and *IRAK3* and *GSK3A* with the greatest correlation according to TCGA and GTEx data (GEPIA coefficient of 0.6 and 0.37, respectively) were identified as significant genes. *CDK1*, which was identified to be upregulated in LNCaP cells compared to PrEC cells, was detected to be negatively co-expressed with *GLI1*. Higher expression of *CDK1* was revealed to be associated with a lower chance of survival in prostate cancer patients during the 25th–110th months approximately (Fig. 5a). These outcomes indicate a tumorigenic role for CDK1 in prostate adenocarcinoma. Besides, screening CDK1 and GLI1 in STRING manifested an experimentally validated interaction between them involved in the positive regulation of cell cycle phase transition (GO:1,901,989). *BID* was downregulated in LNCaP cells and identified to be positively co-expressed with the *BAX* gene. Roughly, after month 75th, the lower expression of *BID* was discovered to be associated with high-risk patients revealing a tumor-suppressor activity for *BID* in prostate cancer (Fig. 5b). Exploring the interactions of BAX and BID proteins in STRING showed an experimentally validated interaction involved in mitochondrial outer membrane permeabilization (GO:0,097,354) and positive regulation of the release of cytochrome c from mitochondria (GO:0,090,200). Lower expression of *IRAK3*, which was illustrated in LNCaP cells through a positive correlation with *GLI1*,

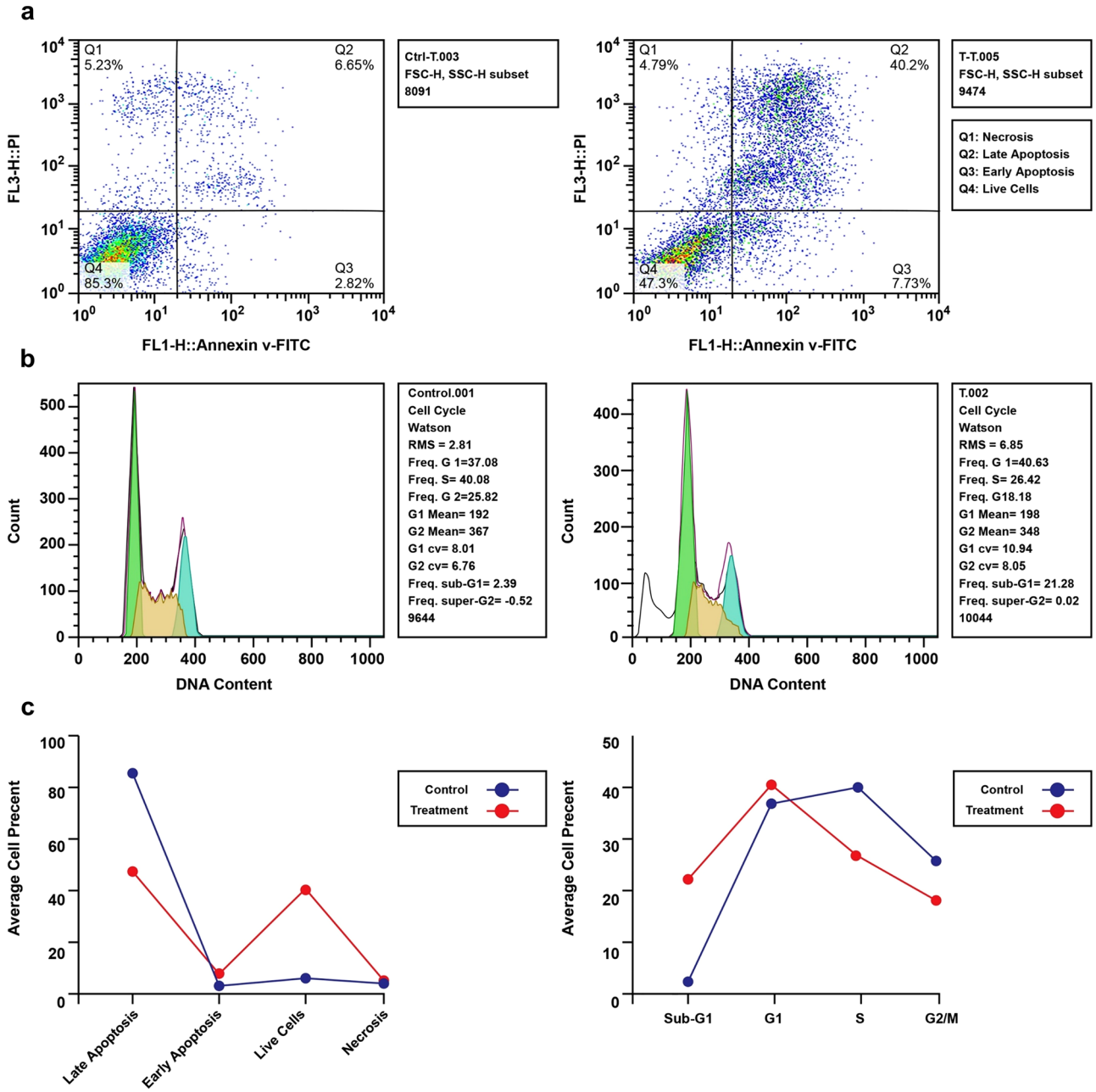


**Figure 2.** Flow cytometry analysis of cell cycle and apoptosis. (**a**) Analysis of apoptosis in LNCaP cells by flow cytometry. Four populations of living, necrotic, early apoptotic, and late apoptotic cells in two groups of control and treated cells are illustrated in density plots, showing the capacity of nanonoscapine in the induction of apoptosis. The bar chart indicates the percentage of cells in the mentioned statuses. (**b**) Analysis of cell cycle by flow cytometry. The quantitative measurements illustrate the impact of nanonoscapine in the induction of cellular arrest in the G2/M phase, followed by the appearance of the sub-G1 population as indicative of apoptosis. (**c**) The apoptosis was induced in the S phase and G2/M cells more than in other cells.

was identified to be fiercely correlated with decreased chances of survival in PRAD patients in the long term after almost month 110th (Fig. 5c) that suggests an anti-tumor activity for IRAK3 in PRAD. Analyzing IRAK3 protein in STRING revealed no direct interactions with GLI1, but contribution in mitotic nuclear division (GO:0,140,014). *GSK3A* downregulation, which was identified as a result of *BAX*-suppressed expression in a positive co-expressive manner, was indicated to be related to the reduced lifetime of PRAD patients between 75 and 110th months (Fig. 5d).

This observation suggested a suppressive activity for *GSK3A* in prostate adenocarcinoma. Moreover, monitoring GSK3A and BAX in STRING indicated no protein interactions, but it was illustrated that GSK3A is involved in the positive regulation of mitochondrial outer membrane permeabilization (GO:1,901,030). Supposing these foundations together with flow cytometry results it can be concluded that induced expression of *GLI1* by nanonoscapine prevents G2 cells from progressing to mitosis by suppressing the expression of *CDK1*

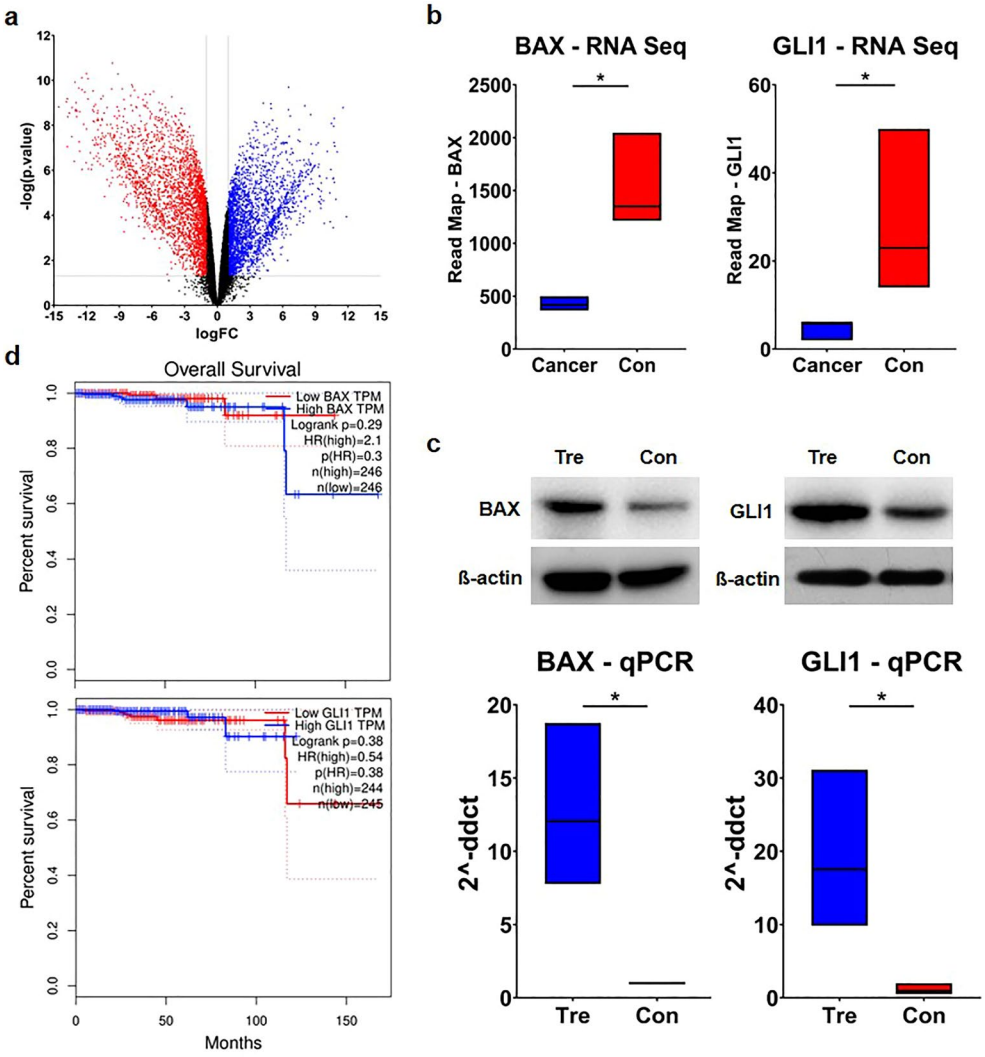


**Figure 3.** Expression analysis of the targeted genes. (**a**) Volcano plot showing the number of significant DEGs in GSE70466, downregulated and upregulated genes are shown in red and blue dots. (**b**) RNA seq read map data manifested the downregulation of *BAX* and *GLI1* in the LNCAP cell line before nanonoscapine treatment. (**c**) After administering nanonoscapine treatment at a dosage of 50 µg/ml for 48 h, a notable increase in the levels of *GLI1* and *BAX* was detected through qRT-PCR and western blot analysis in both the control group (Con) and the nanonoscapine-treated group (Tre). (**d**) The Kaplan Meier plot shows the correlation between the high expression of *BAX* and *GLI1* and the overall survival of prostate cancer patients in GEPIA. TPM is the abbreviation of transcription per million, referring to the expression level of the genes.

and disrupting mitotic cell division by enhancing the expression of *IRAK3*; hence stopping cancerous cells to proliferate. Parallel to this, nanonoscapine treatment upregulates *BAX* and then *BID* and *GSK3A* with the help of which homodimerization of BAX in the outer mitochondrial membrane facilitates the release of cytochrome c (R-HAS-114294) and Smac/DIABLO, which in collaboration with other factors including apoptotic protease activating factor 1 (Apaf-1), procaspase-9, and dATP takes part in the formation of apoptosome complex and activation of caspase-9 which triggers cell death (Fig. 6).

Consequently, nanonoscapine treatment induces the expression of *GLI1* and *BAX*, causing the downregulation of *CDK1* and upregulation of *IRAK3*, *GSK3A*, and *BID* which together with *BAX* and *GLI1* impede prostate adenocarcinoma progression and improves survival chance of patients.

## Discussion

Due to the better delivery chance, blood maintenance, and prospective lower side effects of nano-drugs[18], nanonoscapine was Chosen in the current study to be used instead of noscapine to treat prostate cancer. A previously synthesized and characterized nanonoscapine[24] was analyzed by MTT and demonstrated proper cytotoxicity for cancer cells at the 50 µg/ml concentration in 48 h. Flow cytometry for apoptosis further supported these findings, showing a significant increase in cell death (40.2%) in nanonoscapine-treated cells compared to

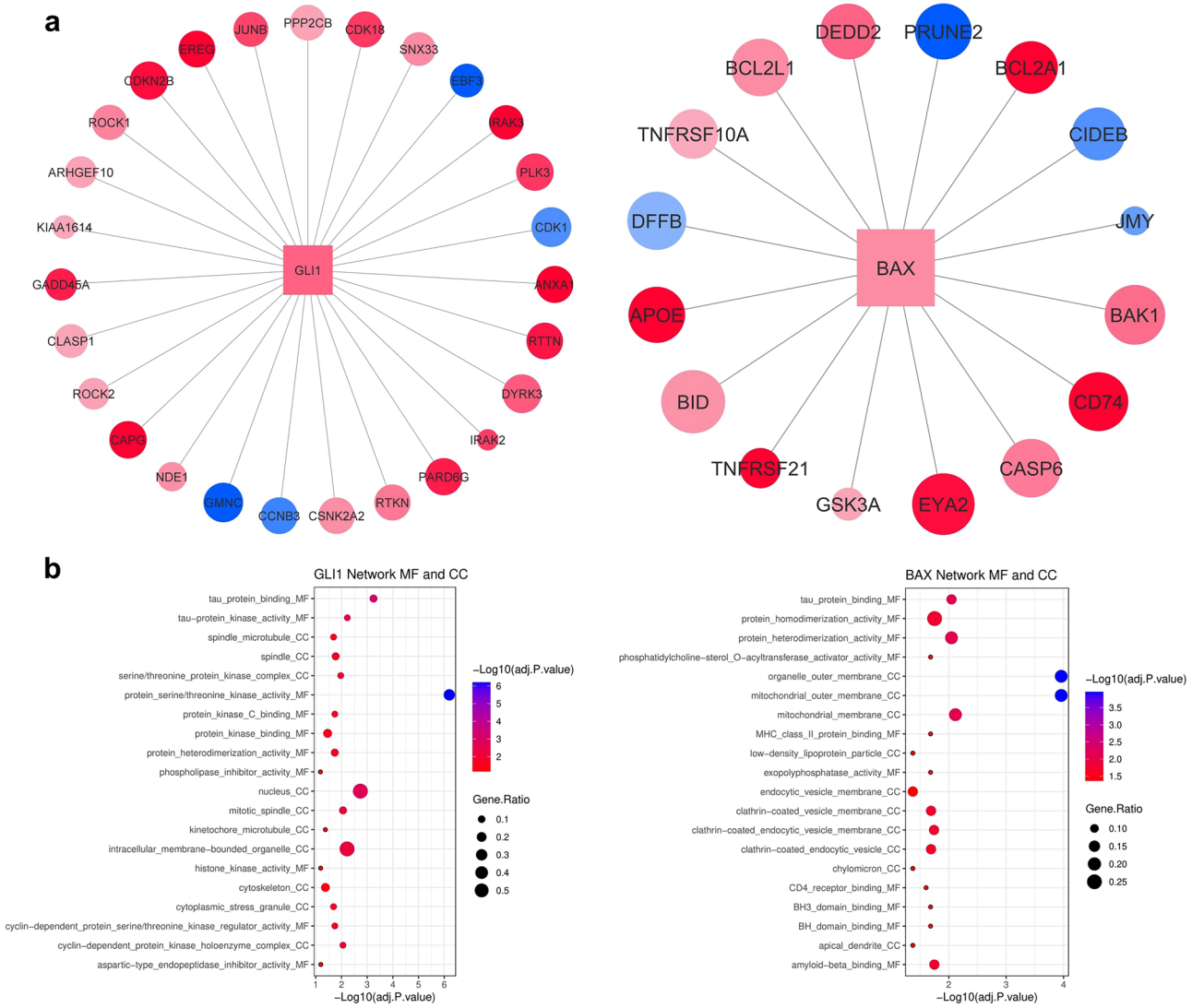


**Figure 4.** Analyzing GLI1 and BAX co-expression network. (**a**) GLI1 and BAX networks were constructed using significant co-expression interactions with cell cycle- and apoptotic-associated genes. Blue and red nodes were upregulated and downregulated genes. The darker the nodes were, the greater the expressions were changed. The bigger the nodes were, the more relevant interactions were detected. (**b**) Network annotation in the aspect of molecular functions and cellular components in PANTHER. Significant gene ontologies were detected with FDR < 0.05.

the control group (6.65%). RNA sequencing, qPCR, and functional bioinformatics analysis indicated *BAX* as a tumor suppressor gene that upregulates confronting nanonoscapine and causes cancer cell apoptosis.

In fact, gene expression analysis and existing literature unveiled, BCL2L1/BCLX, MCL1, BAX, BAK, BAD, BCL2L11/BIM, BBC3/PUMA, PMAIP1/NOXA, BIK and BID as members of the Bcl-2 family proteins expressed in a normal prostate and in PCa[25].

BAX, from the Bcl-2 family and belonging to apoptotic proteins, is one of the central genes responsible for controlling the mitochondria-mediated apoptosis and signaling, which could be activated in response to intrinsic apoptotic signals like chemotherapeutic agents, metabolic stress, and oncogenic stress[26]. Once the activation of BAX has occurred through either direct mode or indirect one, conformational switching is followed by a series of events, including trafficking to mitochondria, aggregation status changes to form a multimer shape, and consequently facilitate the permeabilization of mitochondria membrane, and the release of cytochrome c, which ends up in formation of apoptosome[26]. Apoptosome mediates the activation of initiator caspases such as caspase-9, caspase-8, and caspase-2 which lead to cell death[27].

In breast cancer cell lines, noscapine treatment demonstrated anti-proliferative and apoptotic effects by elevating the BAX/Bcl-2 ratio[28,29]. On colon cancer cell lines, noscapine treatment resulted in the upregulation of Cyt-c and BAX[30,31]. Additionally, in hepatocellular carcinoma, gastric cancer, and leukemic cells, exposure to noscapine showed an escalated ratio of *BAX*/*Bcl2* and suppressed cell growth[32–34].

Furthermore, the anti-tumor activity of noscapine in combination with Cisplatin and another research on xenograft models with H460 lung cancer cells resulted in the upregulation of *BAX*[35,36]. These studies align

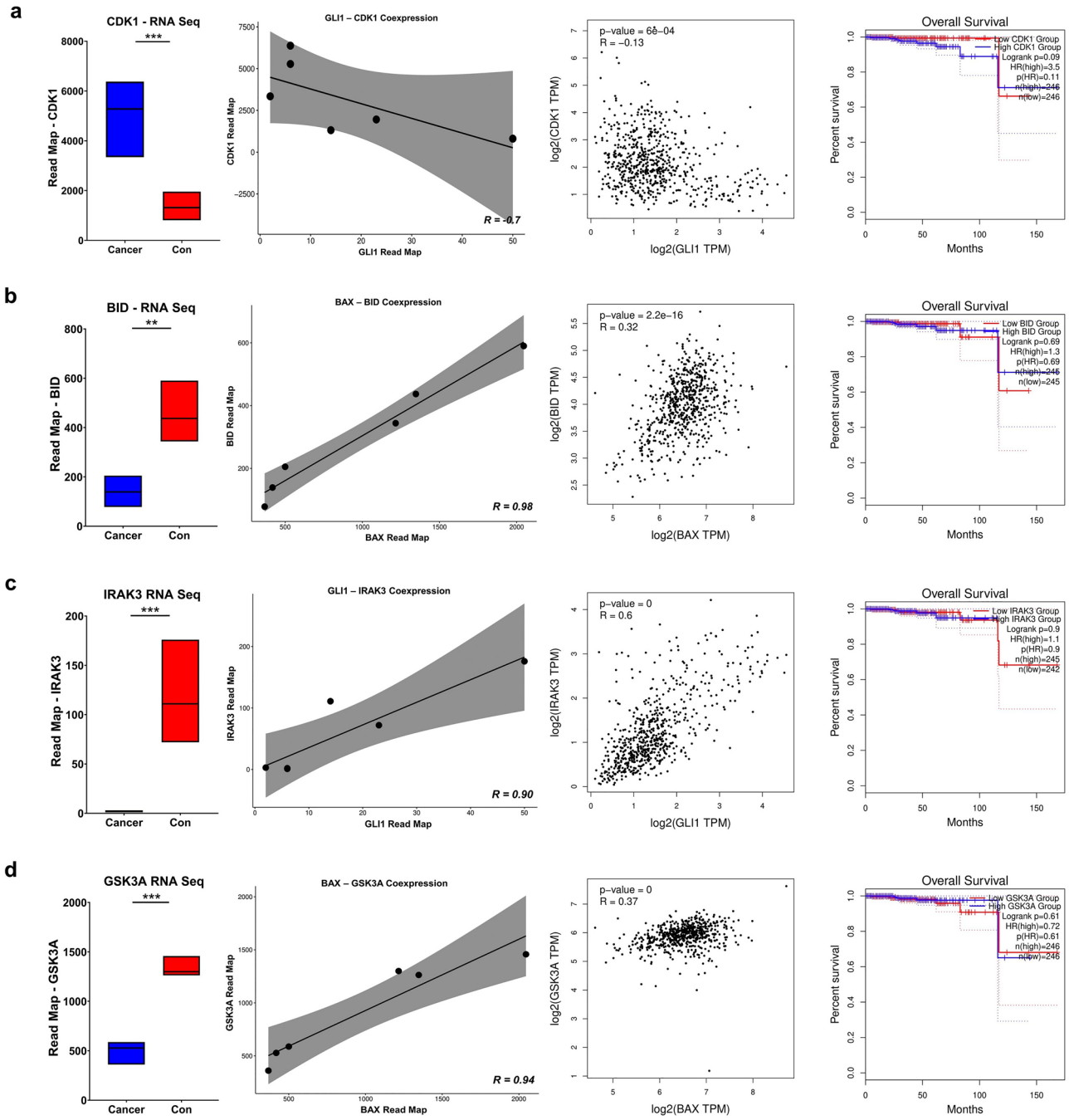


**Figure 5.** Analyzing *CDK1*, *BID*, *IRAK3*, and *GSK3A* using TCGA and GTEx Data. The expression changes in LNCaP and PrEC cells, Pearson correlation calculation in RNA sequencing cohort, Pearson correlation in GEPIA, and Kaplan Meier plot for (**a**) *CDK1*, (**b**) *BID*, (**c**) *IRAK3*, and (**d**) *GSK3A*, respectively.

with our results for nanonoscapine that BAX should be considered a tumor suppressor. Moreover, BAX is also involved in the cascade of autophagy as one of the phenomena with a close correlation to apoptosis, whose regulation is shown to be disrupted in cancer progression[37]. Beclin-1 as one of the central regulators of the network of apoptosis and autophagy, can be released upon cellular stress, and subsequently, lead to increased levels of BAX[38]. It has been shown that in the initial phases of cancer, autophagy could play a protective role though once the tumor has taken root, the cancer cells can take advantage of autophagy[39]. Also in prostate cancer, overexpression of Beclin-1 has been correlated with poor prognosis in patients[40]. Although here we were not focused on autophagy and Beclin-1 as the upstream of BAX, the increase in the expression of BAX was correlated with more apoptosis.

Besides, network analysis showed *GSK3A* and *BID* as essential tumor suppressor genes that are probably upregulated by nanonoscapine treatment through a positive co-expressive manner with *BAX*. Similar to *BAX*, BH3 interacting-domain death agonist (BID) is a member of the Bcl-2 family and manifests pro-apoptotic

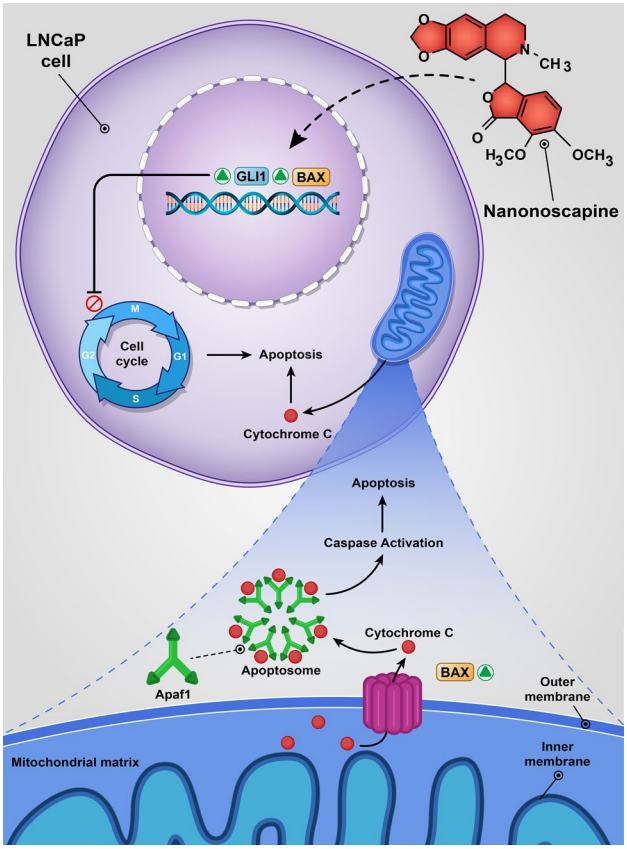


**Figure 6.** Nanonoscapine molecular consequences. Nanonoscapine, after penetrating LNCaP cells, triggers apoptosis through the regulation of a range of various genres, among which *GLI1* and *BAX* are shown in this figure. The increase in the expression of *GLI1* can lead to disruption of the cell cycle and arrest of cells in the G2/M phase. *BAX* raised expression can also cause the oligomerization of this factor in the outer membrane of mitochondria, which helps the formation of apoptosome Apaf1 and cytochrome C by mediating the release of cytochrome C. The formation of apoptosome leads to the activation of caspase, which directly triggers cell death.

functions. BID promotes the mitochondrial outer membrane permeabilization by directly activating BAX or inhibiting anti-apoptotic proteins BCLX and MCL1 to operate; hence, increases the release of cytochrome c which as mentioned earlier causes apoptosis[41]. In line with our results, previously, lower expression of BID in prostate cancer cells, higher expression of BID gene in normal prostate epithelium compared to tumor tissue, and a significant association between the overexpressed BID and higher chances of survival of prostate cancer patients without recurrence have been reported[42]. Likewise, Glycogen synthase kinase-3 α (GSK3A) has been proven to promote cell death through activating signaling pathways and regulating anti- and pro-apoptotic transcription factors which are in line with observations of this study[43]. Taken together, Nanonoscapine treatment promotes cell death in prostate cancer via triggering intrinsic apoptosis signaling pathways by directly upregulating *BAX* and indirectly upregulating *BID* and *GSK3A*.

On the other side, the cell cycle analysis using flow cytometry indicated that the G2/M transition was disrupted, and the cells reached the checkpoint, arrested, and underwent apoptosis. Several previous studies reported that Bcl-2 family members interact with cell cycle machinery and promote G2/M arrest, which is interestingly consistent with our observations[44]. In addition, computer-aided biological annotations showed that upregulation of *GLI1* by nanonoscapine contributes to G2/M arrest via downregulating *CDK1* and might disrupt the mitotic division of nuclear by enhancing *IRAK3* expression. Cyclin-dependent kinases (CDKs) are regulators of the cell cycle and control all aspects of cell division in the G1, S, G2, and mitosis phases[45]. Among these, CDK1 has been detected to promote G2/M transition which is needed for cancerous cells to divide and progress[46]. As a result, the downregulation of *CDK1* due to the upregulation of *GLI1* in a negative co-expressive manner may lead to G2/M phase arrest of cancer cells which was observed in this study in prostate cancer. Conversely, in this research, interleukin-1 receptor-associated kinase-3 (IRAK3) has been identified to interrupt the cell cycle through shattering nuclear division in mitosis. IRAK3 contributes to interleukin-1 signaling which has been shown to activate mitogen-activated protein kinases and transcriptional regulators such as NF-kB[47]. However, recently, the overexpression of IRAK3 in this pathway has been linked to the downregulation of NF-kB via disabling the interactions of IRAK1 and IRAK2 with TRAF6[48]. In a previous article on bladder cancer by Cui et al.[49], upregulation of NF-kB was observed to suppress apoptosis and promote cell cycle progression. Hence, it

can be suggested that in the prostate adenocarcinoma, overexpression of *GLI1* and then *IRAK3* by Nanonoscapine downregulates NF-kB induces apoptosis, and disrupt cell division via impeding nuclear division during mitosis.

*GLI1* is one of the other agents highlighted as a regulator of target genes in the hedgehog signaling pathway[20]. The hedgehog signaling pathway, first discovered in Drosophila, is considered one of the conserved cascades and is imprinted in many developmental events like controlling migration, differentiation, and growth of cells or morphogenesis of organs[50,51]. *GLI1* as a key TF and a terminal effector of the Hedgehog cascade, plays an important role in PCa cell proliferation and EMT. Notably, the activation of Hh/Gli1 signaling is prevalent in PCa is deeply associated with PCa tumorigenesis and the progression toward metastasis[52]. In several studies, the role of *GLI1* in oncogenesis has been reported[53,54]. Despite those mentioned earlier, in this study, the investigation of mRNA indicated an anti-tumor activity for *GLI1*. In an experiment in 2008, it was clear that *GLI1* expression in neural stem cells (NSCs) leads to cell death by causing cell cycle arrest in the G2/M phase[55], which is fascinatingly compatible with our hypothesis. Joost et al.[56] revealed that *GLI1* could act as a regulator of the process of epithelial differentiation, and RNAi-mediated knockdown of this factor led to an increase in cell motility, which was synergized with Tumor Growth Factor-β (TGF-β) expression in simulating an epithelial-to-mesenchymal transition (EMT) that suggest a tumor suppressor role for *GLI1* as well as our study.

## Conclusion

Taken together, our study presents nanonoscapine as a novel and effective therapeutic agent for treating prostate cancer, highlighting its potential to restrict the proliferation of cancer cells and induce apoptosis by regulating the expression of *GLI1* and *BAX* genes. The use of nanotechnology not only improves the bioavailability and delivery of noscapine but also lessens its adverse effects, thereby offering a promising adjunct or alternative to conventional chemotherapy. The significance of this research lies in its contribution to the development of targeted cancer therapies that are more efficient and have fewer side effects, potentially enhancing the quality of life and survival rates for prostate cancer patients. However, several limitations should be appreciated. The in vitro nature of our experiments, while providing valuable insights into the molecular mechanisms of nanonoscapine action, may not fully capture the complexity of in vivo tumor environments. Additionally, the specific focus on the LNCaP cell line, though relevant, does not account for the heterogeneity of prostate cancer and its varied responses to treatment across different patient populations. Further research involving in vivo models and a broader range of prostate cancer cell lines is essential to evaluate our findings and assess the clinical applicability of nanonoscapine. Moreover, comprehensive investigations into the long-term effects and potential toxicity of nanonoscapine in humans are necessary to ensure its safety and efficacy as a therapeutic option.

## Materials and methods

### Nanoprecipitation in the microfluidic reactor

Noscapine saturated in ethanol (Sigma Aldrich®) was injected at room temperature (22 ± 2 °C) into the microfluidic reactor at defined solvent/antisolvent flow rates to produce nanonoscapine. Water was used as the antisolvent system, which was also maintained at ambient temperature (22 ± 2 °C) and contained various concentrations of Tween 40. Very small volumes of liquid were injected using hydrodynamic micropumps (NE 1000 Programmable Syringe Pump). The microreactor used was made of polylactide (polyacetic acid) with an internal diameter of 1 mm and inlet angles of 90°. Accordingly, four different input variables, i.e., the longitudinal exit arm, the angle between the two inlets (inlet angle), the flow rate of the antisolvent, and the Tween 40 concentration were considered in the current study, as it was assumed that they may influence the size and PDI of the produced nanoparticles. The obtained samples were kept at room temperature in the laboratory and then their fresh PDI was measured by DLS. Subsequently, the effects of four input parameters on the size and PDI of the nanosuspension were investigated using the obtained size and PDI data based on the model obtained by ANN modeling[24].

### Cell cultures and treatments

The LNCaP cell line was obtained from the Cell Bank of the Institute Pasteur of Iran, Tehran (#9049). This cell line was cultivated in 100 mm culture dishes at the desired density of DMEM (Gibco, #12,100,061), which was supplemented with 10% fetal bovine serum (FBS, Gibco, #16,000,044), 100 U/ml penicillin, and 100 mg/ml streptomycin (Sigma-Aldrich, #P4333-100ML) at 37 °C and 5% $CO_2$ until reaching 50–70% confluence.

### Cell viability assay

The cell viability assay was performed with MTT (3-[4, 5-dimethylthiazol-2-yl]-2, 5 diphenyl tetrazolium bromide). Upon reaching 70–80% confluence, 5 × 103 cells/well were seeded in a 96-well plate and incubated at 37 °C with 95% air humidity and 5% $CO_2$. When the attachment took place, cells were washed twice with Phosphate-buffered saline (PBS) and starved with serum-free medium (SFM) for 6–12 h. To reach a final 0.1% density of noscapine, the nanoparticles of noscapine were dissolved in DMSO. After starvation, cells were treated with different concentrations of noscapine nanoparticles (12.5, 25, 50, and 100 µM) for 24 and 48 h. Control cells were treated with 1% DMSO[57]. Once the medium had been removed, the cells were washed twice with PBS, 100 ml of MTT (0.5 mg/ml) was added to each well and then incubated for 4 h at 37 °C. After removing the supernatant, to dissolve formazan crystals formed by viable cells after removing media, a volume of 100 µl of DMSO was added. Optical density (OD) was measured at 570 nm with a NanoDrop 1000 Spectrophotometer reader (Wilmington, #291,466). The cell viability was defined as the percent cell viability compared to the vehicle-treated control cells without administering noscapine nanoparticles, which were determined arbitrarily as 100% viability.

## Apoptosis analysis

To monitor the capability of nanonoscapine to induce cell death, apoptosis analysis was performed by flow cytometry. Apoptotic LNCaP cells were detected by Annexin-V staining. LNCaP cells at passage two were treated with $IC_{50}$ of noscapine for 48 h. After the incubation period, the cells were harvested and, to remove the remaining medium were washed in 2 ml of PBS and then centrifuged. The cell's pellet was afterward suspended in 500 µl of IX binding buffer. After dividing and preparing four samples containing propidium iodide (PI), FITC, and PI, Annexin V-FITC, and positive control, the incubation of the cells with 5 µl of Annexin V-FITC was carried out at 4 °C for 15 min in the dark. Flow cytometric analysis was enrolled with BD FACS Calibur (BD bioscience, San Jose, CA). Late apoptotic and dead cells: both Annexin V-positive and PI-positive, early apoptotic cells: Annexin V-positive and PI-negative, and live cells were defined as Annexin V- and PI-negative.

## Cell cycle analysis

To screen the consequence of the nanonoscapine on the cell cycle, flow cytometry was implemented. After harvesting, the cells were washed in ice-cold PBS and vortexed. Before vortexing the cells repeatedly, 50 µl of PBS and 1 ml of 70% ethanol were added to fix the cells. The incubation of cells was then carried out for 2 h at 4 °C, followed by resuspension of the cells with PI Master Mix containing 40 µl of PI, 10 µl RNase, and 950 µl PBS. After 30 min of incubation of cells with the PI master mixture, flow cytometry was performed.

## RNA sequencing analysis

RNA-seq profile of GSE70466, which was established on Illumina HiSeq 2500 platform (GPL16791), was obtained from the GEO database (https://www.ncbi.nlm.nih.gov/geo/) and was subsequently analyzed by BioJupies (http://amp.pharm.mssm.edu/biojupies) based on the Limma R package to determine how *GLI1* and *BAX* were deregulated for prostate cancer cell growth. The expression profile of three chips of LNCaP was compared to three chips of normal prostate epithelial cells (PrEC) (Table S1). Differentially expressed genes (DEGs) were defined by false discovery rate (FDR) < 0.05 and $|Log_2FC| \geq 1$ as the cut-off criteria. To determine the correlation between *GLI1* and *BAX* expression and the survival chance of prostate cancer cases, the Kaplan Meier plot was drawn by GEPIA (http://gepia.cancer-pku.cn/).

## Quantitative real-time PCR

The qPCR was used to measure the expression of *GLI1* and *BAX* after the drug treatment. The total RNA isolation from the LNCaP cell line was carried out using the RNA extraction kit (Roche, #11,828,665,001), based on the manufacturer's guidelines[58]. RNA quality and its concentration were determined using the NanoDrop 1000 Spectrophotometer (Wilmington, #291,466) before cDNA was synthesized. Based on the manufacturer's guidelines, the cDNA synthesis kit was performed using the Easy cDNA synthesis kit (Parstous Biotechnology) and stored at −20 °C. To detect if the expression of *GLI1* and *BAX* were changed by nanonoscapine, Real-time TaqMan qPCR amplification was conducted with a Rotor-Gene 6000 real-time PCR cycler (Qiagen Corbett, Hilden, #R0616300). The data were normalized to the housekeeping *β-actin* gene and fold changes (FC) were calculated according to the $2^{-\Delta\Delta CT}$ expression[59,60]. The primers manufactured by Pishgam company are shown in Table 1. Data were expressed as mean ± standard error of the mean (SEM) and analyzed by the graphed prism (version 8). Groups were compared with an unpaired *t* test and the *p* value of < 0.05 was considered statistically significant.

## Western blot analysis

Western blot analysis was performed by lysing cells using a commercial lysis buffer (Qproteome Mammalian Protein Prep Kit, Qiagen). Total protein (50 µg) was then separated on an SDS-polyacrylamide gel and transferred onto a PVDF membrane (Bio-Rad, USA). The membranes were blocked in a TBS solution containing 20 mM Tris-HCl (pH 7.6), 150 mM NaCl, 0.1% Tween-20, and 5% BSA. Primary antibodies (GLI1; Cell Signaling Technology (CST) 2534, BAX; Santa Cruz, sc-7480, and β-actin; Abcam, ab-1801) were then incubated with the membranes overnight at 4 °C. Following washing, GLI1 and BAX proteins were detected using a horseradish peroxidase (HRP)-conjugated secondary antibody. The signals were visualized using an ECL substrate (GE) and Hyper-film (GE).

| Gene | Primer sequence | Materials concentration | | | |
|---|---|---|---|---|---|
| | | Master Mix | DEPC | Primers | cDNA |
| *GLI1* | F: CCCAATCACAAGTCAGGTTCCT | 4 | 3.5 | 1 | 0.5 |
| | R: CCTATGTGAAGCCCTATTTGCC | | | | |
| *BAX* | F: TGCTTCAGGGTTTCATCCAG | 4 | 4.5 | 0.5 | 0.5 |
| | R: GGCGGCAATCATCCTCTG | | | | |
| *B-Actin* | F: GATCTCCTTCTGCATCCTGT | 4 | 4.5 | 0.5 | 0.5 |
| | R: TGGGCATCCACGAAACTAC | | | | |

**Table 1.** Primer sequences and the concentration of used materials.

## Functional annotations

In order to annotate BAX and GLI1 biological roles in prostate cancer, gene ontology (GO) analysis was performed using the PANTHER database (http://pantherdb.org/), and the significant biological processes (BP), molecular functions (MF), and cellular component (CC) were identified using FDR < 0.05. Afterward, to explore the nanonoscapine consequence on cell cycle and death by affecting BAX and GLI1 as potential targets, all DEGs were analyzed in the PANTHER to identify genes that were involved in the cell cycle (GO:0,007,049), apoptotic process (GO:0,006,915), and hedgehog signaling pathway (P00025). Then, the Pearson correlation was calculated and the correlation coefficient > 0.7 or < −0.7 was considered as the cut-off to discover co-expressing genes. For *BAX* and *GLI1*, apoptotic and cell cycle interacting genes, respectively, were further evaluated using TCGA tumor and normal tissue and GTEx data in the GEPIA database to define significant co-expressed genes. Using such defined edges, two centered networks for cell cycle (GLI1 as the center node) and apoptosis (BAX as the center node) were constructed in Cytoscape (version 3.9.1). Important interacting nodes were identified using the degree and GEPIA co-expression coefficient in GEPIA. Finally, these models were analyzed in PANTHER and STRING databases (https://string-db.org/) to reveal relevant molecular functions and cellular components of these genes according to FDR < 0.05.

## Data availability

The RNA-seq data used in this study is available on GEO with GSE70466. Details on synthesis and characterization tests of the noscapine nanoparticle was published previously[24].

Received: 15 December 2023; Accepted: 25 June 2024
Published online: 16 August 2024

## References

1. Rawla, P. Epidemiology of prostate cancer. *World J. Oncol.* **10**(2), 63–89 (2019).
2. Siegel, R. L., Miller, K. D. & Jemal, A. Cancer statistics, 2020. *CA Cancer J. Clin.* **70**(1), 7–30 (2020).
3. Gann, P. H. Risk factors for prostate cancer. *Rev. Urol.* **4**(Suppl 5), S3–S10 (2002).
4. Grozescu, T. & Popa, F. Prostate cancer between prognosis and adequate/proper therapy. *J. Med. Life* **10**(1), 5–12 (2017).
5. Sathianathen, N. J. *et al.* Landmarks in prostate cancer. *Nat. Rev. Urol.* **15**(10), 627–642 (2018).
6. Di Minno, A. *et al.* 8-hydroxy-2-deoxyguanosine and 8-iso-prostaglandin F2α: putative biomarkers to assess oxidative stress damage following robot-assisted radical prostatectomy (RARP). *J. Clin. Med.* **11**(20), 6102 (2022).
7. Siddiqui, Z. A. & Krauss, D. J. Adjuvant androgen deprivation therapy for prostate cancer treated with radiation therapy. *Transl. Androl. Urol.* **7**(3), 378–389 (2018).
8. Perlmutter, M. A. & Lepor, H. Androgen deprivation therapy in the treatment of advanced prostate cancer. *Rev. Urol.* **9**(Suppl 1), S3-8 (2007).
9. Sandhu, S. *et al.* Prostate cancer. *Lancet* **398**(10305), 1075–1090 (2021).
10. Sekhoacha, M. *et al.* Prostate cancer review: genetics, diagnosis, treatment options, and alternative approaches. *Molecules* **27**(17), 5730 (2022).
11. Rida, P. C. *et al.* The noscapine chronicle: a pharmaco-historic biography of the opiate alkaloid family and its clinical applications. *Med. Res. Rev.* **35**(5), 1072–1096 (2015).
12. Chen, X., Dang, T. T. & Facchini, P. J. Noscapine comes of age. *Phytochemistry* **111**, 7–13 (2015).
13. Zhou, J. *et al.* Minor alteration of microtubule dynamics causes loss of tension across kinetochore pairs and activates the spindle checkpoint. *J. Biol. Chem.* **277**(19), 17200–17208 (2002).
14. Barken, I., Geller, J. & Rogosnitzky, M. Noscapine inhibits human prostate cancer progression and metastasis in a mouse model. *Anticancer Res.* **28**(6A), 3701–3704 (2008).
15. Lasagna, L., Owens, A. H. Jr., Shnider, B. I. & Gold, G. L. Toxicity after large doses of noscapine. *Cancer Chemother. Rep.* **15**, 33–34 (1961).
16. Ohlsson, S. *et al.* Noscapine may increase the effect of warfarin. *Br. J. Clin. Pharmacol.* **65**(2), 277–278 (2008).
17. Madan, J. *et al.* Sterically stabilized gelatin microassemblies of noscapine enhance cytotoxicity, apoptosis and drug delivery in lung cancer cells. *Colloids Surf. B Biointerfaces* **107**, 235–244 (2013).
18. Ma, Y. *et al.* Small molecule nanodrugs for cancer therapy. *Mater. Today Chem.* **4**, 26–39 (2017).
19. Mahmoudian, M. & Rahimi-Moghaddam, P. The anti-cancer activity of noscapine: a review. *Recent Pat Anticancer Drug Discov.* **4**(1), 92–97 (2009).
20. Mahindroo, N., Punchihewa, C. & Fujii, N. Hedgehog-Gli signaling pathway inhibitors as anticancer agents. *J. Med. Chem.* **52**(13), 3829–3845 (2009).
21. Chen, R. & Overholtzer, M. When BAX doesn't kill. *Cell Cycle* **17**(4), 412–413 (2018).
22. Hong, M. *et al.* RNA sequencing: new technologies and applications in cancer research. *J. Hematol. Oncol.* **13**(1), 166 (2020).
23. Ji, F. & Sadreyev, R. I. RNA-seq: basic bioinformatics analysis. *Curr. Protocols Mol. Biol.* **124**(1), e68–e68 (2018).
24. Azarian, M. *et al.* Design and optimization of noscapine nanosuspensions and study of its cytotoxic effect. *J. Biomol. Struct. Dyn.* **37**(1), 147–155 (2019).
25. Ali, A. & Kulik, G. Signaling pathways that control apoptosis in prostate cancer. *Cancers* **13**(5), 937 (2021).
26. Liu, Z. *et al.* Direct activation of bax protein for cancer therapy. *Med. Res. Rev.* **36**(2), 313–341 (2016).
27. Bao, Q. & Shi, Y. Apoptosome: a platform for the activation of initiator caspases. *Cell Death Diff.* **14**(1), 56–65 (2007).
28. Kocak, C., Kocak, F. A. T. M. A., Ozturk, B., Tekin, G. & Vatansev, H. Cytotoxic, anti-proliferative and apoptotic effects of noscapine on human estrogen receptor positive (MCF-7) and negative (MDA-MB-231) breast cancer cell lines. *Bratisl. Lek. Listy* **121**, 43–50 (2020).
29. Quisbert-Valenzuela, E. O. & Calaf, G. M. Apoptotic effect of noscapine in breast cancer cell lines. *Int. J. Oncol.* **48**(6), 2666–2674 (2016).
30. Tian, X. *et al.* Down-regulation of liver-intestine cadherin enhances noscapine-induced apoptosis in human colon cancer cells. *Expert Rev. Anticancer Ther.* **17**(9), 857–863 (2017).
31. Yang, Z. R. *et al.* Noscapine induces mitochondria-mediated apoptosis in human colon cancer cells in vivo and in vitro. *Biochem. Biophys. Res. Commun.* **421**(3), 627–633 (2012).
32. Xu, G. *et al.* Noscapine inhibits human hepatocellular carcinoma growth through inducing apoptosis in vitro and in vivo. *Neoplasma* **63**(5), 726–733 (2016).
33. Liu, M., Luo, X. J., Liao, F., Lei, X. F. & Dong, W. G. Noscapine induces mitochondria-mediated apoptosis in gastric cancer cells in vitro and in vivo. *Cancer Chemother. Pharmacol.* **67**, 605–612 (2011).

34. Heidari, N. *et al.* Apoptotic pathway induced by noscapine in human myelogenous leukemic cells. *Anticancer Drugs* **18**(10), 1139–1147 (2007).
35. Chougule, M., Patel, A. R., Sachdeva, P., Jackson, T. & Singh, M. Anticancer activity of Noscapine, an opioid alkaloid in combination with Cisplatin in human non-small cell lung cancer. *Lung Cancer* **71**(3), 271–282 (2011).
36. Jackson, T., Chougule, M. B., Ichite, N., Patlolla, R. R. & Singh, M. Antitumor activity of noscapine in human non-small cell lung cancer xenograft model. *Cancer Chemother. Pharmacol.* **63**, 117–126 (2008).
37. Qian, S. *et al.* The role of BCL-2 family proteins in regulating apoptosis and cancer therapy. *Front Oncol.* **12**, 985363 (2022).
38. Kang, R. *et al.* The Beclin 1 network regulates autophagy and apoptosis. *Cell Death Differ.* **18**(4), 571–580 (2011).
39. Yun, C. W. & Lee, S. H. The roles of autophagy in cancer. *Int. J. Mol. Sci.* **19**(11), 3466 (2018).
40. Loizzo, D. *et al.* Novel insights into autophagy and prostate cancer: a comprehensive review. *Int. J. Mol. Sci.* **23**(7), 3826 (2022).
41. Slee, E. A., Keogh, S. A. & Martin, S. J. Cleavage of BID during cytotoxic drug and UV radiation-induced apoptosis occurs downstream of the point of Bcl-2 action and is catalysed by caspase-3: a potential feedback loop for amplification of apoptosis-associated mitochondrial cytochrome c release. *Cell Death Differ.* **7**(6), 556–565 (2000).
42. Krajewska, M. *et al.* Expression of Bcl-2 family member Bid in normal and malignant tissues. *Neoplasia* **4**(2), 129–140 (2002).
43. Beurel, E. & Jope, R. S. The paradoxical pro- and anti-apoptotic actions of GSK3 in the intrinsic and extrinsic apoptosis signaling pathways. *Prog. Neurobiol.* **79**(4), 173–189 (2006).
44. Quinn, L. M. & Richardson, H. Bcl-2 in cell cycle regulation. *Cell Cycle* **3**(1), 6–8 (2004).
45. Diril, M. K. *et al.* Cyclin-dependent kinase 1 (Cdk1) is essential for cell division and suppression of DNA re-replication but not for liver regeneration. *Proc. Nat. Acad. Sci.* **109**(10), 3826–3831 (2012).
46. Liao, H., Ji, F. & Ying, S. CDK1: beyond cell cycle regulation. *Aging* **9**(12), 2465–2466 (2017).
47. Guadagno, J. *et al.* Microglia-derived IL-1β triggers p53-mediated cell cycle arrest and apoptosis in neural precursor cells. *Cell Death Dis.* **6**(6), e1779–e1779 (2015).
48. Nguyen, T. H. *et al.* A systematic review and meta-analyses of interleukin-1 receptor associated kinase 3 (IRAK3) action on inflammation in in vivo models for the study of sepsis. *PLOS ONE* **17**(2), e0263968 (2022).
49. Cui, X. *et al.* NF-κB suppresses apoptosis and promotes bladder cancer cell proliferation by upregulating survivin expression in vitro and in vivo. *Sci. Rep.* **7**(1), 40723 (2017).
50. Robbins, D. J., Fei, D. L. & Riobo, N. A. The Hedgehog signal transduction network. *Sci. Signal.* **5**(246), re6 (2012).
51. Mohler, J. Requirements for hedgehog, a segmental polarity gene, in patterning larval and adult cuticle of Drosophila. *Genetics* **120**(4), 1061–1072 (1988).
52. Wang, M. & Huang, W. FOXS1 promotes prostate cancer progression through the Hedgehog/Gli1 pathway. *Biochem. Pharmacol.* **218**, 115893 (2023).
53. Bora-Singhal, N. *et al.* Gli1-mediated regulation of Sox2 facilitates self-renewal of stem-like cells and confers resistance to EGFR inhibitors in non-small cell lung cancer. *Neoplasia* **17**(7), 538–551 (2015).
54. Niewiadomski, P. *et al.* Gli proteins: regulation in development and cancer. *Cells* **8**(2), 147 (2019).
55. Galvin, K. E. *et al.* Gli1 induces G2/M arrest and apoptosis in hippocampal but not tumor-derived neural stem cells. *Stem Cells* **26**(4), 1027–1036 (2008).
56. Joost, S. *et al.* GLI1 inhibition promotes epithelial-to-mesenchymal transition in pancreatic cancer cells. *Cancer Res.* **72**(1), 88–99 (2012).
57. Azarian, M. *et al.* Genotoxicity of noscapine nanosuspension prepared by microfluidic reactors on HepG2 cell line. *Iran. J. Chem. Chem. Eng.* **39**(5), 145–155 (2020).
58. Roche. *life science. Roche*. Feb 2,2018]; Available from: https://www.lifescience.roche.com/global_en/products/high-pure-rna-isolation-kit.html.
59. Livak, K. J. & Schmittgen, T. D. Analysis of relative gene expression data using real-time quantitative PCR and the 2−ΔΔCT method. *Methods* **25**(4), 402–408 (2001).
60. Pfaffl, M. W. A new mathematical model for relative quantification in real-time RT–PCR. *Nucleic Acids Res.* **29**(9), e45–e45 (2001).


## Acknowledgements

We thank the Cancer Biomedical Center for providing instruments and space for the project and Flowcyt Science-Based Company, Tehran, Iran for establishing flowcytometry. Finally, we express gratitude to Mr. Saeed Sadeghi Ghazichaki and Seyedeh Elham Sadeghi for conducting the RT-qPCR and MTT assay. Additionally, our thanks extend to Dr. Maryam Azarian for her contribution to nanoparticle synthesis.

## Author contributions

M.H.D.N: Data curation, Formal analysis, Investigation, Methodology, Validation, Visualization, Writing—original draft. R. H., Conceptualization, Writing—original draft. R.A.D, and P.G.T and M.M. Data curation, Investigation, Methodology, Writing—original draft, S.T., Conceptualization, Investigation, Methodology, Writing—review & editing and supervised the study.

## Funding

Partial financial support was received from the Cancer Biomedical Center, Tehran, Iran.

## Competing interests

The authors declare no competing interests.

## Additional information

**Supplementary Information** The online version contains supplementary material available at https://doi.org/10.1038/s41598-024-65968-4.

**Correspondence** and requests for materials should be addressed to S.T.